Available online at www.sciencedirect.com

SCIENCE DIRECT®

Journal of Organometallic Chemistry 665 (2003) 218–225

Journal of Organometallic Chemistry

www.elsevier.com/locate/jorganchem

Synthesis, NMR and structural studies of cluster derivatives derived from reactions of 1,2,3-triphenyl-1,2,3-triphosphaindan with $[Os_3(CO)_{10}(\mu\text{-}H)_2]$

Siau-Gek Ang*, Xinhua Zhong, How-Ghee Ang

Department of Chemistry, National University of Singapore, Singapore 119260, Singapore

Received 21 August 2002; accepted 30 October 2002

Abstract

Reactions of 1,2,3-triphenyl-1,2,3-triphosphaindan (**I**) with $[Os_3(CO)_{10}(\mu\text{-}H)_2]$ at various conditions afford a series of osmium carbonyl cluster derivatives: an open bent-chain trinuclear cluster $[Os_3(CO)_9\{\mu_3\text{-}\eta^3\text{-}PPhC_6H_4(PPh)_2\}]$ (**1**), a di-substituted bridged trinuclear cluster $[Os_3(CO)_{10}\{\mu\text{-}1,3\text{-}\eta^2\text{-}C_6H_4(PPh)_3\}]$ (**2**), a 1,3-linked bis-trinuclear hydride cluster $[\{(\mu\text{-}H)_2Os_3(CO)_9\}_2\{\mu\text{-}1,3\text{-}\eta^2\text{-}\{C_6H_4(PPh)_3\}]$ (**3**), an open bent-chain trinuclear cluster $[Os_3(CO)_7\{C_6H_4(PPh)_3\}\{\mu_3\text{-}\eta^3\text{-}\{(PPh)_2C_6H_4PPh\}]$ (**4**), and a closed trinuclear cluster $[(\mu\text{-}H)Os_3(CO)_8\{C_6H_4(PPh)_3\}\{\mu\text{-}\eta^3\text{-}\{C_6H_4(PPh)_2PC_6H_4\}]$ (**5**). All the compounds obtained have been fully characterized by spectroscopic methods (IR, FABMS, ^1H- and ^{31}P-NMR spectroscopy), and the molecular structures of **3**, **4**, **5** are established by X-ray crystallography.

Keywords: Osmium cluster; Triphosphaindan; ^{31}P-NMR; Crystal structures

1. Introduction

Considerable attention has been paid to the subject of cluster-ligand interactions, from which an insight into the behavior of these molecules on metal surfaces in chemisorption and heterogeneous catalysis may be obtained [1–3]. The reactions of homocyclopolyphosphines $(PR)_n$ (R = Ph [4a,4b,4c], Et [4c,4d,4e], CF_3 [4f], or ^{t}Bu [5]; $n = 4$ or 5) with triosmium and triruthenium carbonyl clusters have been extensively studied. However, the same does not apply to the heterocyclopolyphosphines. For the investigated cyclocarbophosphine ligand 1,2,3-triphenyl-1,2,3-triphosphaindan (**I**), its reactions with iron [6,7], ruthenium [8a] and acetonitrile activated triosmium carbonyl clusters (i.e. $[Os_3(CO)_{12-n}NCMe)_n]$, $n = 1$ or 2) [8b] afforded a wide range of ligand bonding modes on the cluster framework. This cyclocarbophosphine has been found to be able to act as a mono- and bi-dentate bridging ligand through two outer phosphorus atoms where the ring framework remains intact. In some instances, the ligand undergoes ring rupture with the cleavage of one or two intracyclic P–P bond(s) or even intracyclic P–C bonds under forcing reaction conditions to afford $PPhC_6H_4(PPh)_2$, $PPhC_6H_4PPh$, PPh, and C_6H_4 fragment ligand units.

In this paper, we extend our studies on the reaction of **I** with triosmium hydride cluster $[Os_3(CO)_{10}(\mu\text{-}H)_2]$, where several new cluster derivatives are obtained. These include the rarely encountered triosmium cluster $[Os_3(CO)_7\{C_6H_4(PPh)_3\}\{\mu_3\text{-}\eta^3\text{-}\{(PPh)_2C_6H_4PPh\}]$ (**4**) containing a pentacoordinated osmium atom adopting a square pyramidal configuration, and the first reported cyclopolyphosphine complexed cluster $[(\mu\text{-}H)Os_3(CO)_8\{C_6H_4(PPh)_3\}\{\mu\text{-}\eta^3\text{-}C_6H_4(PPh)_2PC_6H_4\}]$ (**5**) with a phenyl group bonded to phosphorus involved in an *ortho*-metallation reaction.

---

* Corresponding author. Tel.: +65-687-23564

E-mail addresses: sciangsg@nus.edu.sg (S.-G. Ang), maszx@nus.edu.sg (X. Zhong).

0022-328X/02/$ - see front matter © 2002 Elsevier Science B.V. All rights reserved.
PII: S0022-328X(02)02120-4

2. Results and discussion

2.1. Reactivity

The reactions of 1,2,3-triphenyl-1,2,3-triphosphaindan (**I**) with $[Os_3(CO)_{10}(\mu\text{-}H)_2]$ is shown in Scheme 1. When **I** reacts with $[Os_3(CO)_{10}(\mu\text{-}H)_2]$ in an equimolar ratio at 100 °C in toluene, an open bent-chain trinuclear cluster coordinated with the cleaved ligand $[Os_3(CO)_9\{\mu_3\text{-}\eta^3\text{-}PPhC_6H_4(PPh)_2\}]$ (**1**), and a di-substituted bridged trinuclear cluster $[Os_3(CO)_{10}\{\mu\text{-}1,3\text{-}\eta^2\text{-}C_6H_4(PPh)_3\}]$ (**2**) are obtained in 9 and 21% yields, respectively. Cluster **1** is a known compound, which was obtained previously via the reaction of $[Os_3(CO)_{11}(NCMe)]$ with **I** [8b]. When the above reaction is performed using a ligand to cluster ratio of 1:2, a 1,3-linked bis-trinuclear hydride cluster $[\{(\mu\text{-}H)_2Os_3(CO)_9\}_2\{\mu\text{-}1,3\text{-}\eta^2\text{-}\{C_6H_4(PPh)_3\}]$ (**3**) is formed in 27% yield. When the reaction is carried out with a ligand to cluster ratio of 2:1, an open bent-chain trinuclear cluster $[Os_3(CO)_7\{C_6H_4(PPh)_3\}\{\mu_3\text{-}\eta^3\text{-}\{(PPh)_2C_6H_4PPh\}]$ (**4**), and a closed trinuclear cluster $[(\mu\text{-}H)Os_3(CO)_8\{C_6H_4(PPh)_3\}\{\mu\text{-}\eta^3\text{-}\{C_6H_4(PPh)_2PC_6H_4\}]$ (**5**) are obtained in 5 and 8% yields, respectively. Cluster **4** contains an open bent-chain trinuclear metal skeleton with an intact ligand **I** coordinated at a terminal metal atom, and another ligand fragment with a P–P bond cleavage capping the three metal atoms using a $\mu_3\text{-}\eta^3$-coordination mode. This cluster is an electron-deficient species with a rarely encountered pentacoordinated osmium atom adopting a square pyramidal configuration. In cluster **5**, one osmium atom of the triosmium triangle is coordinated by an intact ligand, and the edge involving the other two osmium atoms is bridged over by another ligand via the coordination of two outer phosphorus atoms. The phenyl group on the central uncoordinated phosphorus atom is involved in an *ortho*-metallation reaction with one of these Os atoms to form an M–C bond with migration of the hydrogen atom to bridge over a M–M edge.

All the new compounds obtained are formulated, and fully characterized by spectroscopic (FABMS, ^1H- and ^{31}P-NMR) techniques (Table 1), in addition, ^{31}P–^{31}P COSY-90-NMR spectra are recorded for clusters **4** and **5**.

2.1.1. Cluster $[Os_3(CO)_{10}\{\mu\text{-}1,3\text{-}\eta^2\text{-}C_6H_4(PPh)_3\}]$ (**2**)

As observed for the free ligand [9], the $^{31}P\{^1H\}$-NMR spectrum shows an AX_2 spin pattern (see Table 1). From the ^{31}P-NMR spectrum, we can deduce that the fused P_3C_2-ring framework of ligand **I** remains intact in the cluster. The equivalency of the two outer phosphorus atoms in the ligand implies that either they or the central phosphorus are coordinated at the cluster. Taken together with the other spectroscopic results, we can conclude that ligand **I** in cluster **2** bonds to the

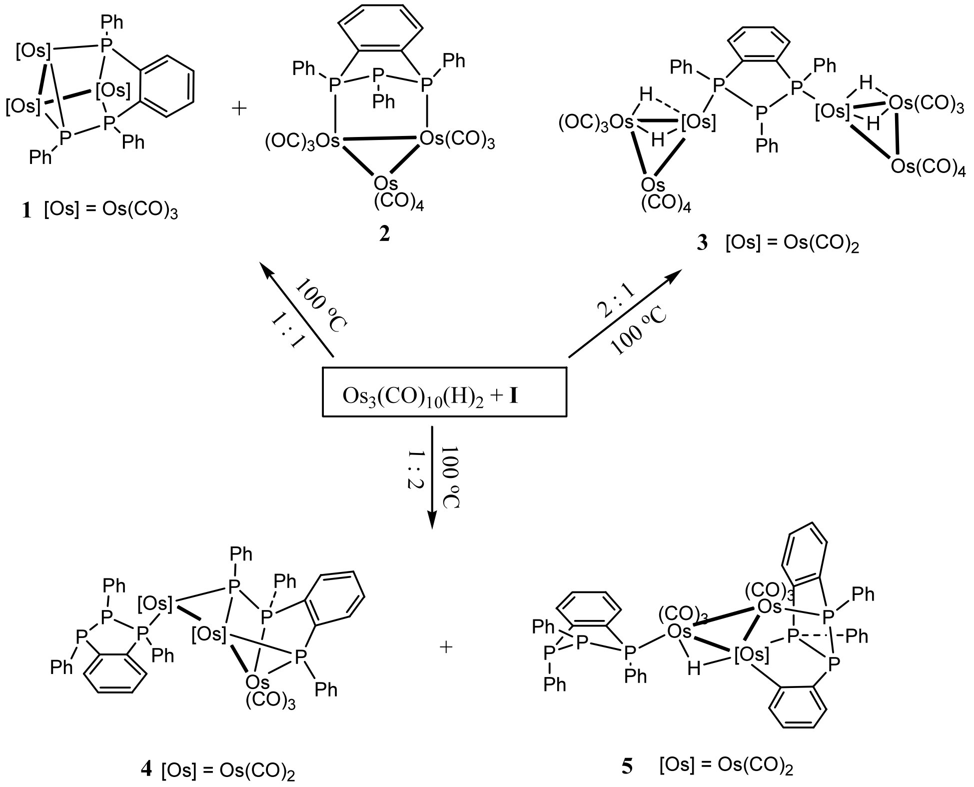

Scheme 1.

Table 1
Spectroscopic data for clusters **1**–**5**

	IR, ν(CO) (cm^{-1}) [a]	^1H-NMR, δ (J Hz) [b]	$^{31}P\{^1H\}$-NMR, δ (J Hz) [b]	MS (m/z) [c]
1	2071s, 2047vs, 2013vs, 2006s, 1990w, 1978w,1963w, 1937w	6.8–8.3 (m, Ph)	32.0 (dd, 217.4, 7.6, 1P); −9.3 (dd, 217.4, 26.7, 1P); −107.4 (dd, 26.7, 7.6, 1P)	1223 (1223)
2	2097s, 2035w, 2017vs, 1980w, 1962w, 1943w	6.9–8.2 (m, Ph)	120.1(t, 175.5, 1P, P^2); −43.5(d, 175.5, 2P, P^1, P^3)	1251 (1251)
3	2109w, 2091m, 2073w, 2055s, 2038w, 2014vs, 1988w	6.9–8.4 (m, 20H, Ph) −10.9 (m, 4H, M–H)	43.7(d, 267.1, P^1,P^3); −35.0 (t, 267.1, P^2)	2050 (2050)
4	2045s, 1990vs, 1958w, 1941w	6.3–8.6 (m, Ph)	70.8(s, P^6); 35.0(dd, 264.0, 117.2, P^1); 22.6(d, 213.6, P^4); 13.8(d, 259.4, P^3); 8.0(dd, 213.6, 117.2, P^5); −42.9(dd, 264.0, 259.4, P^2)	1567 (1567)
5	2082w, 2005s, 1980w, 1951w	6.2–8.4 (m, 37H, Ph) −16.8 (m, 1H, M–H)	111.0(dd, 171.8, 114.1, P^2); 21.8(dd, 114.1, 57.1, P^1/P^3); 19.3(d, 279.2, P^6); 15.9(d, 265.6, P^4); 11.5(dd, 171.8, 57.1, P^1/P^3); −45.6 (dd, 279.2, 265.6, P^5)	1595 (1595)

[a] In CH_2Cl_2.
[b] In $CDCl_3$ with $SiMe_4$ for ^1H and 85% H_3PO_4 for ^{31}P as references.
[c] Simulated values are given in parentheses.

triosmium triangle via the coordination of two outer phosphorus atoms and adopts a μ-1,3-η^2 coordination mode. This bonding mode for ligand **I** has been encountered in a formerly reported cluster (which we label as *cis*-**2**) with the same formula but with different ^{31}P-NMR spectroscopic properties ($^{31}P\{^1H\}$-NMR for *cis*-**2**: 48.8(t, $^1J_{PP} = 253.0$ Hz, 1P); −2.4(d, $^1J_{PP} = 253.0$ Hz, 2P)) [8b]. We deduce that **2** and *cis*-**2** are a pair of configurational isomers. For the coordination mode adopted by these two isomers, only the uncoordinated central phosphorus atom is possibly able to change its configuration due to the inversion of the lone pair of electrons and the phenyl group (Ph^2) attached at it. In the structure of *cis*-**2**, Ph^2 has a *cis*-configuration with respect to the neighboring phenyl groups, thus, in **2**, we deduce that Ph^2 should adopt a *trans*-configuration. The proposed structure for cluster **2** is shown in Fig. 1.

Infrared analysis gives further support to the proposed structure for cluster **2**. The similarities in the IR absorption patterns for the reported configurational isomer pair $[Os_3(CO)_{10}\{\mu\text{-}1,3\text{-}\eta^2\text{-}(CPh)_2(PPh)_3\}]$ [10], with Ph^2 adopting a *cis*- or *trans*-configuration with respect to its neighboring phenyls, parallel those in the isomeric **2** and *cis*-**2** (i.e. the only significant differences lie in the shape and position of the strongest peaks) (IR spectra are available in the supplementary material). For comparison, the IR spectra for the two pairs of configurational isomers are listed in Table 2. Obviously, the steric crowding among phenyl groups in the ligand ring is more pronounced in *cis*-**2** than in **2**. In *cis*-**2,** however, this overcrowding is at least partly compensated by the lower repulsion between Ph^2 and $Os(CO)_3$ units as they are pointing in opposite direction. Isomeric *cis*-**2** and *trans*-**2** cannot be interconverted in the solution state even at 95 °C in their toluene solutions (confirmed by ^{31}P-NMR spectral data). Similiar isomeric polyphosphine complexed clusters (e.g. $(PPh)_5$-cyclo [4b], and $(PPh)_4CH_2$-cyclo [11]) have been previously reported.

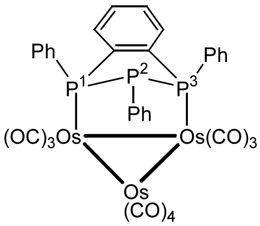

Fig. 1. Proposed structure for cluster **2**.

2.1.2. Cluster $[\{Os_3(CO)_9(\mu\text{-}H)_2\}_2\{\mu\text{-}1,3\text{-}\eta^2\text{-}\{C_6H_4(PPh)_3\}\}]$ (**3**)

The ^{31}P-NMR spectrum of **3** also shows a first-order AX_2 spin pattern. From the ^{31}P-NMR spectrum, we know that the P–P bonds of ligand **I** in the cluster remain intact, and the two outer phosphorus atoms have equivalent chemical environments. From all the spectroscopic data we can deduce that in **3** the two outer phosphorus of **I** are linked to two triosmium hydride cluster units.

In order to confirm the proposed structure, X-ray single crystal diffraction was done. The resulting mole-

Table 2
IR ν(CO) for two pairs of configurational isomers $[Os_3(CO)_{10}\{\mu\text{-}1,3\text{-}\eta^2\text{-}L\}]$

Ligand	Ph^2 orientation	ν(CO) in solution (cm^{-1})
I	*cis*	2093s, 2033w, 2020s, 2008vs, 1977w, 1962w, 1948w
	trans	2097s, 2035w, 2017vs, 1980w, 1962w, 1943w
$(CPh)_2(PPh)_3$	*cis*	2095m, 2034w, 2019m, 2012vs, 1982ww, 1964w, 1955w
	trans	2098m, 2034w, 2018vs, 1985w, 1965w, 1952w

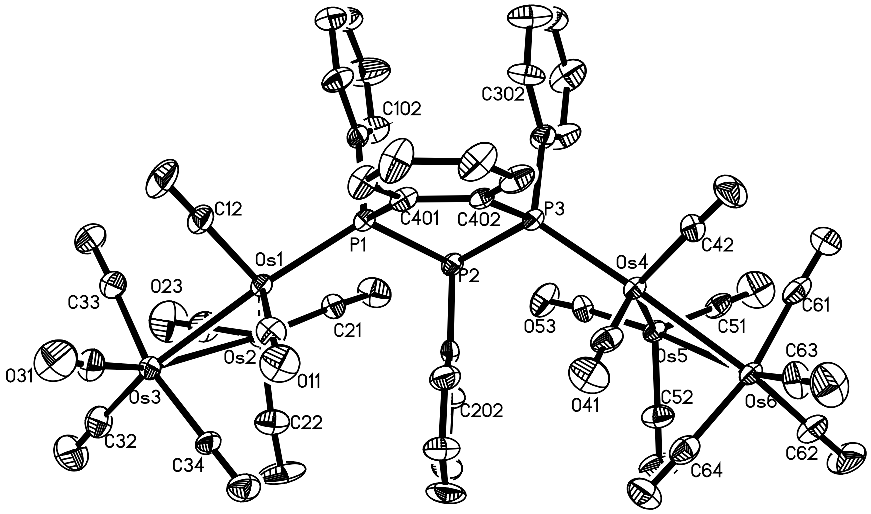

Fig. 2. ORTEP view of cluster **3**.

cular structure is shown in Fig. 2 together with the atomic labeling scheme. Important bond lengths and angles are listed in Table 3. In cluster **3**, the ligand **I** links two discrete $\{Os_3(CO)_9(\mu\text{-}H)_2\}$ units using the two outer phosphorus atoms by the substitution of a carbonyl group from each of the parent clusters $[Os_3(CO)_{10}(\mu\text{-}H)_2]$. Each of the hydrido bridged triosmium carbonyl units $\{Os_3(CO)_9(\mu\text{-}H)_2\}$ has a geometry similar to that of the parent cluster $[Os_3(CO)_{10}(\mu\text{-}H)_2]$ [12,13] with one M–M bond (Os(1)–Os(2), and Os(4)–Os(5)) being exceptionally short (2.6932(7), 2.6956(7) Å) and bridged over by two hydrides (not located crystallographically). The geometry of the coordinated ligand is the same as that of free ligand with all the phenyl groups attached on phosphorus atom *trans* to the neighboring phenyl groups [14]. The fused P_3C_2-ring is no longer co-planar with P(2) out of the plane at a distance of 0.13 Å.

2.1.3. Cluster $[Os_3(CO)_7\{C_6H_4(PPh)_3\}\{\mu_3\text{-}\eta^3\text{-}\{(PPh)_2C_6H_4PPh\}]$ (**4**)

The $^{31}P\{^1H\}$-NMR spectrum of **4** exhibits a first-order spin pattern with six resonances of equal intensity (see Table 1). The COSY-90 ^{31}P-NMR spectrum is also recorded (available in the supplementary material). From the molecular structure, it is reasonable to assign the singlet resonance at 70.8 ppm to P(6) and the resonance at −42.9 ppm, which contains two ^1J couplings, to P(2). The resonances at 35.0 and 13.8 ppm should then correspond to P(1) and P(3), respectively. For the resonance signal of P(1), besides the ^1J coupling with P(2), there is also a long-range coupling with another phosphorus atom. This long-range coupling possibly arises from the ^2J coupling between P(1) and P(5). Hence, we can assign the resonance at 8.0 ppm to P(5), and the resonance at 22.6 ppm to P(4). The large $^2J_{PMP}$ coupling (117.2 Hz) between P(1) and P(5) (while those between P(6) and P(4) or P(6) and P(5) cannot be observed) is possibly due to the P–M–P bond angle. From the X-ray structure (see Chart 1), we know the investigated PMP bond angles are: ∠P(1)–Os(1)–P(5), 158.16(5)°; ∠P(5)–Os(2)–P(6), 95.46(6)°; and ∠P(4)–Os(3)–P(6), 77.71(6)°. P(1) and P(5) are *trans* to each other in a osmium centered square pyramidal configuration environment, while P(6) and P(4) or P(6) and P(5) are *cis* to each other. This observation accords with the general rule that the magnitude for $^2J(XMY)_{trans}$ is usually greater than that for $^2J(XMY)_{cis}$ [15].

Table 3
Selected bond lengths (Å) and angles (°) for cluster **3**

Bond lengths	
Os(1)–Os(2)/Os(4)–Os(5)	2.6932(7)/2.6956(7)
Os(1)–Os(3)/Os(4)–Os(6)	2.8134(7)/2.8124(6)
Os(2)–Os(3)/Os(5)–Os(6)	2.8200(8)/2.8126(7)
P(1)–Os(1)/P(3)–Os(4)	2.347(3)/2.347(3)
P(1)–P(2)/P(2)–P(3)	2.213(4)/2.215(4)
Bond angles	
Os(1)–Os(2)–Os(3)/Os(4)–Os(5)–Os(6)	61.32(2)/61.36(2)
Os(1)–Os(3)–Os(2)/Os(4)–Os(6)–Os(5)	57.12(2)/57.27(2)
Os(2)–Os(1)–Os(3)/Os(5)–Os(4)–Os(6)	61.56(2)/61.37(2)
P(1)–P(2)–P(3)	94.1(2)

The molecular structure of **4** is shown in Fig. 3 together with the atomic labeling scheme, and the selected bonding parameters are listed in Table 4. Two independent molecules with similar geometries exist in the asymmetric unit cell of cluster. Only one molecule is

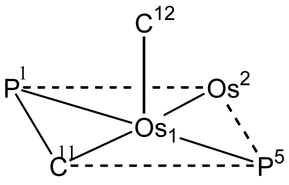

Chart 1. The configuration of Os(1) in **4**.

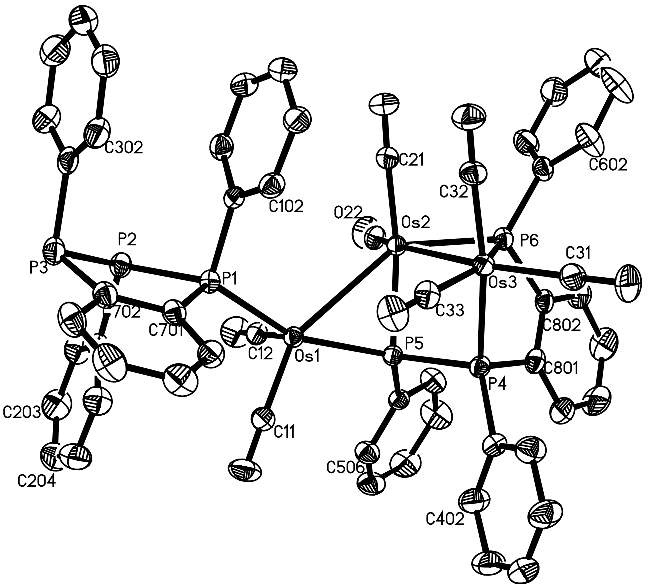

Fig. 3. ORTEP view of cluster **4**.

discussed here (Molecule 1, Table 4). The metal core of the cluster is an open bent-chain of three osmium atoms with a angle of 94.45(3)° (i.e. ∠Os(1)Os(2)Os(3)). The two M–M edges are bridged respectively by two phosphido phosphorus atoms P(5) and P(6) derived from the breakage of a P–P bond in one ligand molecule. The two terminal osmium atoms Os(1) and Os(3) are also coordinated to two phosphine phosphorus atoms P(1) and P(4), respectively. One of the most interesting features of the cluster is that both Os(2) and Os(3) are six-coordinated (including two M–M bonds), and adopt nearly octahedral configuration, while Os(1) is only five-coordinated, and adopts a rarely seen square pyramidal geometry with P(1), C(11), P(5), and Os(2) defining the square base, C(12) located on the apex (see Chart 1), and with an unsaturated valence electron number of 16. The carbonyl group (CO(12)) at the apex of this square pyramid has a much longer Os–C distance (Os(1)–C(12), 1.952(6) Å) than the other Os–C bond in the base plane (Os(1)–C(11), 1.867(6) Å). It is also apparently longer than the average Os–C distance of all the other carbonyls in the cluster (average 1.901 Å). This is because this apex carbonyl has no σ-donator in *trans* position, and thus cannot participate in effective back donation π-bonding. The two phosphorus P(1) and P(5) on the base plane are mutually *trans*, which is why the $^2J_{POsP}$ coupling constant is large (117.2 Hz). The Os–Os distances, (particularly Os(1)–Os(2), 3.0793(8) Å) are apparently longer than those of the parent triosmium triangle cluster $Os_3(CO)_{12}$ (average 2.877 Å) [16], which contrasts with the general rule that in the case of electron-poor systems, electron deficiency is usually compensated by the formation of multiple bonds [17].

Table 4
Selected bond lengths (Å) and angles (°) for cluster **4** (two independent molecules per asymmetric unit cell)

	Molecule 1	Molecule 2
Bond lengths		
Os(1)–Os(2)	3.0793(8)	3.0697(8)
Os(1)–P(1)	2.344(2)	2.354(2)
Os(2)–P(5)	2.372(2)	2.360(2)
Os(3)–P(4)	2.381(2)	2.371(2)
P(1)–P(2)	2.209(2)	2.209(3)
P(4)–P(5)	2.195(2)	2.179(2)
Os(2)–Os(3)	2.9428(7)	2.9677(9)
Os(1)–P(5)	2.346(2)	2.328(2)
Os(2)–P(6)	2.296(2)	2.300(2)
Os(3)–P(6)	2.350(2)	2.348(2)
P(2)–P(3)	2.215(3)	2.212(2)
Bond angles		
Os(1)–Os(2)–Os(3)	94.45(3)	94.46(3)
P(1)–P(2)–P(3)	94.40(9)	96.0(1)

2.1.4. Cluster $[(\mu\text{-H})Os_3(CO)_8\{1\text{-}C_6H_4(PPh)_3\}\{\mu_2\text{-}\eta^3\text{-}\{C_6H_4(PPh)_2PC_6H_4\}]$ (5)

The $^{31}P\{^1H\}$-NMR spectrum of cluster **5** shows a first-order spin pattern with six resonance signals of equal intensities (see Table 1). In order to establish the coupling relationship among these six resonance signals, a COSY-90 ^{31}P-NMR spectrum is recorded (available in the supplementary material). In the COSY spectrum, the resonances at 111.0, 21.8 and 11.5 ppm are observed to couple to each other, and so they must arise from one ligand moiety. The resonance at −45.6 ppm couples with both resonances at 19.3 and 15.9 ppm in the other ligand moiety. From the molecular structure, we know that there are two ligand **I** moieties in the cluster. The spin patterns for the resonances at 19.3, 15.9 and −45.6 ppm are very similar to those of mono-substituted cluster $[Os_3(CO)_{11}(C_6H_4(PPh)_3)]$ reported previously [8b]. It is reasonable to assign these three resonances to the phosphorus atoms (P(4), P(5), and P(6)) of the ligand which adopts a η^1-coordination mode in the cluster. The resonance at 15.9 ppm is assigned to the coordinated phosphorus atom P(4) on the basis of reduction in the magnitude of the $^1J_{PP}$ coupling constant on complexation [15]. For the three remaining resonances, the resonance at 111.0 ppm should correspond to the central phosphorus atom P(2), while those at 21.8 and 11.5 ppm correspond to P(1) and P(3) but cannot be precisely assigned.

The molecular structure of cluster **5** is depicted in Fig. 4 together with the atomic labeling scheme, and selected structural parameters are listed in Table 5. The metal core of the cluster constitutes a triangular geometry. Os(2) is coordinated to an intact ligand **I** through an equatorial position, while the other metal–metal edge (Os(1)–Os(3)) is bridged by the two outer phosphorus atoms P(1) and P(3) of another ligand **I**. The phenyl

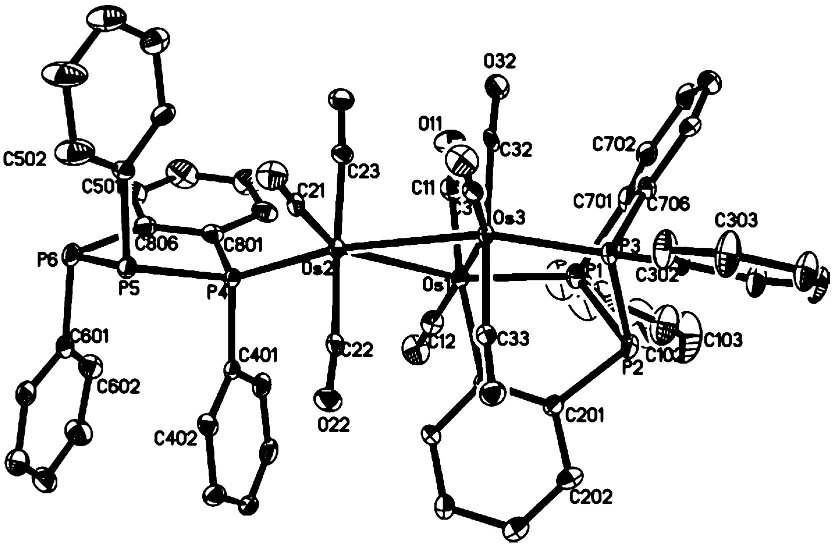

Fig. 4. ORTEP view of cluster **5**.

Table 5
Selected bond lengths (Å) and angles (°) for cluster **5**

Bond lengths			
Os(1)–Os(2)	3.0792(5)	Os(1)–Os(3)	2.9151(5)
Os(2)–Os(3)	2.8614(5)	P(1)–Os(1)	2.304(2)
P(3)–Os(3)	2.306(2)	P(4)–Os(2)	2.345(2)
P(1)–P(2)	2.202(4)	P(2)–P(3)	2.277(4)
P(4)–P(5)	2.199(4)	P(5)–P(6)	2.209(4)
C(206)–Os(1)	2.165(9)		
Bond angles			
Os(1)–Os(2)–Os(3)	58.64(2)	Os(2)–Os(3)–Os(1)	64.42(2)
Os(3)–Os(1)–Os(2)	56.95(2)	P(1)–P(2)–P(3)	82.0(2)
P(4)–P(5)–P(6)	94.2(2)		

group on the central phosphorus atom P(2) is *ortho*-metalleted with Os(1), forming a M–C σ bond (Os(1)–C(206), 2.165(9) Å). Due to the *ortho*-metallation of Ph^2, the P(1)P(2)P(3) moiety [P(2) out of the original P_3C_2 plane at a distance of 0.37 Å] is distorted more severely than the P(4)P(5)P(6) moiety [P(5) out of the original P_3C_2 plane at a distance of 0.16 Å]. *Ortho*-metallation, which leads to the cleavage of a C–H bond, and the formation of a M–C σ bond, is commonly observed in the thermolysis of $[Os_3(CO)_{11}L]$, where L is a tertiary phosphine or arsine [18,19]. To date there is no report of such reactions in the polyphosphine coordinated osmium clusters, so this case may well serve as the first example.

Although the spectroscopically detected hydride was not located crystallographically, we can tentatively assign it to be bridging across the longest Os(1)–Os(2) edge. The unusual orientation of equatorial ligands gives further support for the determination of the position for the hydride. The Os(1)–Os(2) edge is associated with a much larger Os–Os–CO angle (∠C(12)–Os(1)–Os(2), 113.5(3)°) than the other two edges (∠C(21)–Os(2)–Os(3), 93.3(3)°; ∠C(31)–Os(3)–Os(2), 98.8(3)°). Apparently, the larger CO–Os–Os angles are derived from the crowding resulting from the extra hydrido ligand over the M–M edge.

3. Experimental

3.1. General

All reactions described above were carried out in vacuo (around 10 mbar) using double-tube-reaction vessels equipped with Teflon taps. Analytical grade solvents were purified by distillation over appropriate drying agents, and in a nitrogen atmosphere prior to use. Products were separated by TLC using laboratory-prepared 20 × 20 cm glass plates coated to thickness of 0.3 mm with Merck Kieselgel $60F_{254}$ silica gel using mixtures of dichloromethane and hexane in various proportions as eluents. The starting materials $[Os_3(CO)_{12})]$, $[Os_3(CO)_{10}(\mu\text{-}H)_2]$, and ligand **I** ($C_6H_4(PPh)_3$) were prepared by literature methods [20,21,8]. Samples for elemental analysis were evacuated at vacuo (around 10 mbar) at 60 °C for 2 h beforehand. Elemental analysis was carried out at the Microanalytical Laboratory, Department of Chemistry, National University of Singapore. Infrared spectra were recorded as solution in 0.5 mm KBr cell on a Bio-Rad FTS-165 spectrometer, ^1H- and ^{31}P-NMR spectra on Bruker 300 or 500 MHz Fourier-Transform spectrometers and mass spectra on a Finnigan MAT 95 instrument by the fast atom bombardment technique, using α-nitrobenzyl alcohol or thioglycerol as the matrix solvent.

All single crystals for X-ray diffraction analysis were obtained by slow evaporation of a saturated CH_2Cl_2–hexane solution at −20 °C for several days or by slow diffusion of hexane into a dichloromethane solution at −20 °C. Crystal data and details of the measurement for clusters **3**–**5** are given in Table 6. Diffraction intensities were collected at 293 K on a Siemens CCD SMART diffractometer using graphite-monochromated Mo–K_α radiation ($\lambda = 0.71073$ Å), and ω–2θ scan technique. The diffraction data were corrected for absorption by using the SADABS program. The structures were solved by direct methods, and the refinement was by the full-matrix least-squares method with all non-hydrogen atoms refined anisotropically. All computations were carried out using a SHELXTL IRIS version 5.04 software package [22].

3.2. *Reactions of [$Os_3(CO)_{10}(\mu\text{-}H)_2$] with $C_6H_4(PPh)_3$ (**I**)*

3.2.1. *At equimolar ratio*

The compound [$Os_3(CO)_{10}(\mu\text{-}H)_2$] (150 mg, 0.18 mmol) and **I** (70 mg, 0.18 mmol) were placed in the inner tube of a double-tube-reaction vessel and degassed under vacuo. Freshly distilled toluene (10 cm^3) was placed in the outer tube of the reaction vessel. After degassing with three freeze–pump–thaw cycles, the solvent was then transferred to the inner tube with the reactants. The reaction vessel and the reactants inside were heated in a 100 °C oil bath. The color of the reaction mixture changed to bright red in a few minutes. The reaction system was stirred at this temperature for 5 h. After cooling to room temperature (r.t.), the resultant red reaction mixture was transferred into a 50 ml round bottom flask and evaporated to dryness under reduced pressure. The red residue was dissolved in a minimum volume of dichloromethane and separated by TLC using CH_2Cl_2–hexane (1/3, v/v) as eluent. Three bands of yellow **1** ($R_f = 0.54$, 18 mg, 9%), and red **2** ($R_f = 0.46$, 43 mg, 21%) together with an uncharacterized product were eluted consecutively (Found for **2**: C, 33.01; H, 1.28; P, 6.86. Calc. for $C_{34}H_{19}O_{10}Os_3P_3$: C, 32.64; H, 1.52; P, 7.43%).

3.2.2. *At cluster to ligand ratio of 2:1*

The reaction conditions were similar to those of 3.2.1 above. 200 mg (0.23 mmol) of [$Os_3(CO)_{10}(\mu\text{-}H)_2$] reacted with 47 mg (0.12 mmol) of **I** in 10 ml of freshly distilled toluene in vacuo at a 100 °C oil bath for 5 h to afford a red solution. After removal of solvent, the red residue was dissolved in dichloromethane, and subjected to preparative TLC for separation using CH_2Cl_2–hexane (1/3, v/v) as eluent. Most of the residue could not be developed and retained at the base line. Only one major band of red compound **3** ($R_f = 0.48$, 64 mg, 27%) was eluted and characterized (Found for **3**: C, 25.02; H, 1.42; P, 4.06. Calc. for $C_{42}H_{23}O_{18}Os_6P_3$: C, 24.59; H, 1.12; P, 4.54%).

3.2.3. *At cluster to ligand ratio of 1:2*

The reaction conditions were similar to those of 3.2.1 above. 140 mg (0.16 mmol) of [$Os_3(CO)_{10}(\mu\text{-}H)_2$] reacted with 130 mg (0.32 mmol) of **I** in 10 ml of freshly distilled toluene in vacuo at 100 °C for 5 h to afford a red solution. After removal of solvent, the red residue was dissolved in dichloromethane and subjected to preparative TLC for separation using dichloromethane-hexane (3/7, v/v) as eluent. Eight bands were developed on the plates, but only the first two bands of red cluster **4** ($R_f =$

Table 6
Summary of crystallographic data for clusters **3**–**5**

Compound	**3**	**4**	**5**
Formula	$C_{42}H_{23}O_{18}Os_6P_3 \cdot 0.5\ CH_2Cl_2$	$C_{55}H_{38}O_7Os_3P_6$	$C_{56}H_{37}O_8Os_3P_6 \cdot 0.5CH_2Cl_2$
Formula weight	2092.18	1567.27	1636.74
Crystal system	Monoclinic	Triclinic	Monoclinic
Space group	$P2(1)/n$	$P\bar{1}$	$P2(1)/c$
a (Å)	12.5777(2)	15.9992(1)	13.6456(2)
b (Å)	17.6431(3)	16.6797(2)	11.9313(2)
c (Å)	24.5284(3)	23.9675(3)	37.0648(3)
α (°)		92.43(3)	
β (°)	90.78(2)	101.68(3)	97.807(1)
γ (°)		110.63(3)	
V (Å^3)	5442.6(1)	5817(2)	5979(2)
Z	4	4	4
μ (mm^{-1})	14.155	6.749	6.615
Reflections measured	49 415	52 273	37 072
Unique reflections	13 739	27 605	14 521
R_{int}	0.0777	0.0291	0.0552
$[I > 2\sigma(I)]$	$R_1 = 0.0512$, $wR_2 = 0.1265$	$R_1 = 0.0342$, $wR_2 = 0.0879$	$R_1 = 0.0637$, $wR_2 = 0.1347$
All data	$R_1 = 0.0925$, $wR_2 = 0.1379$	$R_1 = 0.0525$, $wR_2 = 0.0967$	$R_1 = 0.0890$, $wR_2 = 0.1444$
S(F^2)	1.029	1.100	1.133
Temperature (K)	293(2)	293(2)	293(2)

0.65, 13 mg, 5%), and red cluster **5** ($R_f = 0.57$, 21 mg, 8%) were characterized (Found for **4**: C, 41.83; H, 2.08; P, 11.28. Calc. for $C_{55}H_{38}O_7Os_3P_6$: C, 42.15; H, 2.44; P, 11.86%. Found for **5**: C, 42.48; H, 2.49; P, 11.12. Calc. for $C_{56}H_{38}O_8Os_3P_6$: C, 42.16; H, 2.40; P, 11.65%).

4. Supplementary material

Crystallographic data for the structural analysis have been deposited with the Cambridge Crystallographic Data Centre, CCDC nos. 182133–182135 for compounds **3**, **4** and **5**, respectively. Copies of this information may be obtained free of charge from The Director, CCDC, 12 Union Road, Cambridge CB2 1EZ, UK (Fax: +44-1223-336033; e-mail: deposit@ccdc.cam.ac.uk or www: http://www.ccdc.cam.ac.uk). The figures of IR spectra for **2** and ^{31}P–^{31}P COSY-90-NMR spectra for **4** and **5** are available upon request from the authors.

Acknowledgements

We thank the National University of Singapore for financial support and for a Research Scholarship (to X.H.Z.).

References

[1] E.L. Mutterties, Science 196 (1977) 839.

[2] E.L. Mutterties, T.N. Rhodin, E. Band, C.F. Brucker, W.R. Pretzer, Chem. Rev. 79 (1979) 91.

[3] R.D. Adams, F.A. Cotton, Catalysis by Di-, and Polynuclear Metal Cluster Complexes, VCH, New York, 1998.

[4] (a) H.G. Ang, L.L. Koh, Q. Zhang, J. Chem. Soc. Dalton Trans. (1995) 2757;
(b) H.G. Ang, S.G. Ang, Q. Zhang, J. Chem. Soc. Dalton Trans. (1996) 3843;
(c) H.G. Ang, S.G. Ang, Q. Zhang, J. Chem. Soc. Dalton Trans. (1996) 2773;
(d) H.G. Ang, S.G. Ang, W.L. Kwik, Q. Zhang, J. Organomet. Chem. 485 (1995) C10;
(e) H.G. Ang, S.G. Ang, Q. Zhang, Phosphorus, Sulfur Silicon Relat. Elem. 110 (1996) 145;
(f) H.G. Ang, K.W. Aug, S.G. Ang, A.L. Rheingold, J. Chem. Soc. Dalton Trans. (1996) 3131.

[5] (a) B.F.G. Johnson, T.M. Layer, J. Lewis, P.R. Raithby, W.T. Wong, J. Chem. Soc. Dalton Trans. (1993) 973;
(b) E. Charalambous, L. Heuer, B.F.G. Johnson, J. Lewis, W.S. Li, M. McPartlin, A.D. Massey, J. Organomet. Chem. 468 (1994) C9.

[6] R.B. King, R.H. Reimann, Inorg. Chem. 15 (1976) 184.

[7] E.P. Kyba, K.L. Hassett, B. Sheikh, J.S. Mckennis, R.B. King, R.E. Davis, Organometallics 4 (1985) 994.

[8] (a) S.G. Ang, X.H. Zhong, H.G. Ang, Phosphorus, Sulfur Silicon Relat. Elem. 117 (2002) 1463;
(b) S.G. Ang, X.H. Zhong, H.G. Ang, J. Chem. Soc. Dalton Trans. (2001) 1151.

[9] F.G. Mann, A.J.H. Mercer, J. Chem. Soc. Perkin Trans. I (1972) 1631.

[10] H.G. Ang, S.G. Ang, X. Wang, J. Chem. Soc. Dalton Trans. (2000) 3429.

[11] S.G. Ang, X.H. Zhong, H.G. Ang, Inorg. Chem. 41 (2002) 3791.

[12] M.R. Churchill, F.J. Hollander, J.P. Hutchinson, Inorg. Chem. 16 (1977) 2697.

[13] V.F. Allen, R. Manson, P.B. Hitchcock, J. Organomet. Chem. 140 (1977) 297.

[14] J.J. Daly, J. Chem. Soc. A (1966) 1020.

[15] C.J. Jameson, in: J.G. Verkade, L.D. Quinn (Eds.), Phosphorus-31-NMR Spectroscopy in Stereochemical Analysis: Theoretical Considerations: Spin–Spin Coupling (Chapter 6), VCH Publishers, Deerfield Beach, FL, 1987.

[16] M.R. Churchill, B.G. DeBoer, Inorg. Chem. 16 (1977) 878.

[17] G.M. Guillermo, Cluster Chemistry: Introduction to the Chemistry of Transition Metal and Main Group Element Molecular Clusters (Chapter 2), Springer-Verlag, Berlin, Heidelberg, 1993.

[18] (a) C.W. Bradford, R.S. Nyholm, J. Chem. Dalton Trans. (1973) 529;
(b) G.J. Gainsford, J.M. Guss, P.R. Ireland, R. Manson, C.W. Bradford, R.S. Nyholm, J. Organomet. Chem. 40 (1972) C70.

[19] (a) A.J. Deeming, R.E. Kimber, M. Underhill, J. Chem. Soc. Dalton Trans. (1973) 2589;
(b) A.J. Deeming, M. Underhill, J. Chem. Soc. Dalton Trans. (1973) 2727;
(c) A.J. Deeming, I.P. Rothwell, M.B. Hursthouse, J.D. Backer-Dirks, J. Chem. Soc. Dalton Trans. (1981) 1879.

[20] B.F.G. Johnson, J. Lewis, Inorg. Synth. 13 (1972) 93.

[21] H.D. Kaesz, Inorg. Synth. 28 (1990) 238.

[22] SHELXTL, version 5.1, Bruker AXS, Inc., Madison, WI, 1997.